# Structure–Property Relationships in Acrylate/Epoxy Interpenetrating Polymer Networks: Effects of the Reaction Sequence and Composition

**Joseph R. Nowers,[1,2] Joseph A. Costanzo,[1] Balaji Narasimhan[1]**

[1]*Department of Chemical and Biological Engineering, Iowa State University, 2035 Sweeney Hall, Ames, Iowa 50011-2230*
[2]*3M Company, 900 Dayton Avenue, Ames, Iowa 50010*

Received 5 August 2006; accepted 2 November 2006
DOI 10.1002/app.25748
Published online in Wiley InterScience (www.interscience.wiley.com).

**ABSTRACT:** Interpenetrating polymer networks (IPNs) of poly(ethylene glycol) 200 diacrylate and diglycidyl ether of bisphenol A were formed over a range of compositions and with different reaction sequences. We controlled the reaction sequence by thermally initiating the cationic epoxy polymerization, photoinitiating the free-radical acrylate polymerization, and changing the processing order. The reaction was monitored by attenuated total reflectance Fourier transform infrared spectroscopy, photo differential scanning calorimetry. and modulated differential scanning calorimetry (mDSC). The glass-transition temperature was estimated from mDSC. Mechanical and rheological tests provided the strength and hardness of the materials. Morphology and phase separation were explored with optical and scanning electron microscopy. All of the physical properties were dependent on IPN composition. Some properties and the morphology were dependent on the reaction sequence. Significant differences in glass-transition temperature were observed at the same composition but with different reaction sequences. Even with minimal structure, correlations existed between the morphology and material properties with partially phase-separated samples exhibiting maximum damping. The rapid reaction allowed minimal phase separation, yet different reaction sequences resulted in significantly different properties. This systematic study indicated that the relationships between phase morphology, processing, and the physical properties of IPNs are complex and not predictable *a priori*. © 2007 Wiley Periodicals, Inc. J Appl Polym Sci 104: 891–901, 2007

**Key words:** interpenetrating networks (IPN); mechanical properties; processing; structure-property relations

## INTRODUCTION

Interpenetrating polymer networks (IPNs) are formed from two or more polymers when at least one of the multifunctional monomers is polymerized in the presence of the other crosslinked polymer.[1] To form a single phase, either the solubilities of the components must be compatible over the range of the compositions and monomer conversions or the polymerization rate must be faster than the dissolution rate.[2] More homogeneous IPNs are formed with faster reaction rates and when the reactions are close to simultaneous.[3] If the system completely phase separates, a polymer composite is formed. If partial phase separation occurs, which is more likely, a series of phases of varying composition are formed.

IPNs have been used in a wide range and variety of applications. Urethane/acrylate systems have been extensively studied and are commonly used in vibration-damping applications. The morphology and phase domain sizes of urethane/acrylate IPNs were studied as a function of the reaction sequence.[4] Larger domains were formed when the acrylate was reacted first. The reaction sequence was controlled in this study by thermal polymerization of the urethane and photopolymerization of the acrylate. Cellulose acrylate was added to a polycarbonate to form IPNs that remained transparent and had improved damping properties over the polycarbonate homopolymer.[5] An extensive study of a urethane/polyester network allowed modeling and the attainment of a variety of material properties.[6] The complex nature of the model reflected the complexity of the interactions in the network. A number of epoxy amine/acrylate[7–10] and epoxy anhydride/acrylate[11] systems have been studied. In one study, optically clear networks were formed that were fully compatible when the epoxy content was greater than 50%. This was evidenced by single peaks in rheological studies (i.e., tan $\delta$ plots).[8] In another study, maxima in the energy absorbed and Young's modulus ($E$) were observed at intermediate compositions. Full IPNs had improved properties relative to semi-IPNs. The decline in semi-IPN material properties at some compositions was attributed to microphase separation.[9] In all of these studies, the polymerization rate decreased for both polymers, and

*Correspondence to:* B. Narasimhan (nbalaji@iastate.edu).


©2007 Wiley Periodicals, Inc.
WILEY InterScience® DISCOVER SOMETHING GREAT

the activation energies increased during full IPN formation. Dean and Cook[11] performed mechanical analysis that exhibited two phases when the methacrylate was cured first but one phase when the epoxy was cured first. The curing sequence was controlled by photopolymerization of the methacrylate and thermal reaction of the epoxy anhydride. The final conversions of each monomer in these systems also depended on the reaction sequence. This dependence was attributed to vitrification, topological constraints, or phase separation.

The physical properties of IPNs are often enhanced over those of the individual polymers and blends of the polymers[12]. Examples of properties that have been studied include tensile yield stress, $E$, compressive modulus, storage modulus ($G'$),[13,14] glass-transition temperature ($T_g$),[11,15,16] hardness,[6] and swelling.[17,18] The morphology of IPNs has been characterized by optical microscopy,[19] scanning electron microscopy (SEM),[13,20] transmission electron microscopy,[21] and atomic force microscopy.[13,15,17,22] These studies have also shown that reaction conditions and sequence impact the final microstructure of IPNs.

To engineer IPNs with specific properties, a detailed understanding of the relationships beyond the effect of composition during IPN formation is required. The reaction sequence and reaction rates of the network significantly impact the morphology and material properties. A fundamental understanding of the relationships between microstructure, phase behavior, processing conditions, composition, and physical properties is required to provide a framework for engineering material performance.

In this study, epoxy/acrylate IPNs were formed over a range of compositions and by changes in the reaction sequence. The conversion was estimated by modulated differential scanning calorimetery (mDSC) and attenuated total reflectance (ATR) Fourier transform infrared (FTIR) spectroscopy. The mechanical and rheological properties were measured as a function of temperature. The morphology of the IPNs at different compositions and reaction sequences was studied by optical microscopy and SEM. The relationships among the morphology, physical properties, composition, and processing conditions were systematically explored.

## EXPERIMENTAL

### Materials

Poly(ethylene glycol) 200 diacrylate (PEG200DA), a multifunctional acrylate (marketed under the trade designation SR-259), was purchased from Sartomer (Exton, PA), and bisphenol A/ephichlorohydrin epoxy resin [diglycidyl ether of bisphenol A (DGEBA)], a multifunctional epoxy (marketed under the trade designation EPON 828), was purchased from Resolution Performance Products (Houston, TX). The acrylate was polymerized with α,α-dimethoxy-α-phenylacetophenone (DMPA), a free-radical photoinitiator (marketed under the trade designation Irgacure 651), from Ciba Specialty Chemicals (Basel, Switzerland). The epoxy was reacted with a thermally activated cationic catalyst, a proprietary ammonium antimony hexafluoride (marketed under the trade designation XC-7231), from King Industries (Norwalk, CT). The chemical structures of the acrylate, epoxy, and photoinitiator are shown in Figure 1. All materials were used as received.

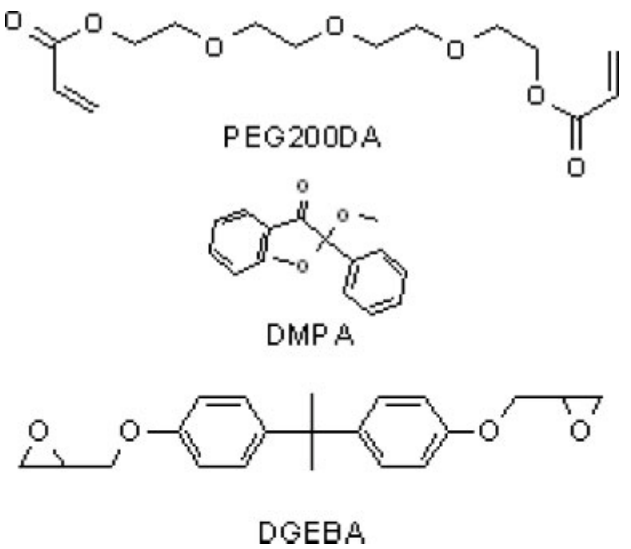


**Figure 1** Chemical structures of the acrylate (PEG200DA), the photoinitiator (DMPA), and the epoxy (DGEBA).

### Methods

The materials were weighed and mixed at room temperature. The photoinitiator was miscible with the diacrylate and was added in darkened room conditions at 1 wt % of the diacrylate. The DGEBA epoxy was heated in a water bath to 50°C before the catalyst was added. XC-7231 was added at 1 wt % of the epoxy. Blends of epoxy and acrylate were made at acrylate weight fractions of 0.25, 0.50, and 0.75 and were miscible. The materials were stored in dark bottles.

Rectangular stainless steel molds were fabricated following ASTM D 5279 with 10 columns and four rows for rheometric analysis.[23] The rectangle size was reduced to 60.325 × 12.5 × 3.175 $mm^3$. Dogbone-shaped stainless steel molds were fabricated following ASTM D 638 type IV with 10 columns and four rows for tensile testing.[24] The molds were bolted to a steel plate. Between the plate and the mold, a foam spacer and a silicone release coated liner was added. The molds were sprayed with a fluorocarbon mold release agent before sample preparation. Pure acrylate sam-

ples were made at slightly thinner dimensions to cure the acrylate and to prevent stress fracturing during curing.

### Epoxy first

Samples were prepared by two reaction sequences; epoxy first and acrylate first. For the epoxy-first reaction sequence, the mold cavities were filled with blends containing 25, 50, and 75 wt % acrylate. The molds were placed in an oven at 100°C for 60 min. The temperature was then raised to 125°C for 25 min. The molds were removed from the oven and passed under a Fusion UV Systems (Gaithesburg, MD) test stand configured with a VPS 6 power supply and irradiator with a D bulb. To minimize stress fracture, the samples were passed through the test stand at 25 fpm at 25% power 20 times, then at 50% power 5 times, and then once at 100% power. The samples were removed from the molds. Samples were placed back in the oven at 125°C for 95 min and then at 160°C for 120 min to complete the epoxy reaction. The pure epoxy samples were made in a similar manner except that the samples were removed from the mold after 60 min at 100°C.

### Acrylate first

The acrylate-first reaction samples were made similarly to the epoxy samples, except the order was reversed. The mold cavities were filled with the blends and passed through the test stand at the same speed and power sequence as discussed previously. Samples were removed from the molds and then baked in the oven at 100°C for 1 h, 120°C for 2 h, and 160°C for 2 h. The total time in the oven at a given temperature was the same for all samples (both acrylate and epoxy).

### Conversion by FTIR

An FTIR spectrophotometer with diamond ATR (Thermo Nicolet,Waltham, MA) was used to measure IR absorption. A smooth spot was created on the samples by scrapping or polishing to ensure good contact with the ATR crystal.

Acrylate conversion was determined by measuring the absorbance at 1635 $cm^{-1}$. To standardize the measurements, a baseline from 1554 to 1658 $cm^{-1}$ was used. Fractional conversion ($a$) was estimated as shown in Eq. (1):

$$a = 1 - \left(\frac{I_{\text{sample},1635}}{I_{\text{monomer},1635}}\right) \quad (1)$$

Here $I_{\text{sample}}$ and $I_{\text{monomer}}$ refer to sample and monomer absorbance respectively.

A similar approach was used to estimate epoxy conversion. The absorbance at 914 $cm^{-1}$ was used to indicate ring-opening polymerization. A baseline from 883 to 927 $cm^{-1}$ was used in most cases. In a few instances, the baseline was adjusted to prevent negative absorbances. A correction factor was added to the absorbances to account for instrument drift and variability in measurements. The peak for correction was at 1508 $cm^{-1}$, which was due to the absorbance of the aromatic ring. A baseline from 1328 to 1554 $cm^{-1}$ was used to adjust the peak height. The conversion was calculated according to Eq. (2), which includes the reference absorbance correction:

$$a = 1 - \left(\frac{I_{\text{sample},914}}{I_{\text{monomer},914}}\right)\left(\frac{I_{\text{monomer},1508}}{I_{\text{sample},1508}}\right) \quad (2)$$

### Acrylate conversion by photo differential scanning calorimetry (pDSC)

Samples (~ 2–5 mg) were removed from the dogbone or rectangle specimens for pDSC measurements and placed in standard differential scanning calorimetry (DSC) pans. A thermal analyzer (DSC Q1000, TA Instruments, New Castle, DE) with a photocalorimetry accessory (PCA) UV light accessory was used to react the samples and study the kinetics and physical properties. To check for residual photoreaction, which was assumed to be due to the acrylate, the sample was stabilized at 30°C and then irradiated at 50 $mW/cm^2$ for 3 min.

### mDSC

mDSC was used for further thermal analysis of post-reacted samples. A 2–5 mg sample was removed from the physical property specimens and placed into a standard DSC pan and sealed. The sample was equilibrated at −50°C. The temperature was ramped at 10°C/min to 300°C and modulated at 1°C/min every 30 s. The sample was held at 300°C for 30 s and ramped back down to −50°C at the same ramp and modulation rate.

The DSC traces were further processed with the Universal Analysis program (TA Instruments). Inflections in the reversible heat flow curves were used to estimate the $T_g$ values. Typically, an initial $T_g$ was found on the upward temperature ramp, and the final or ultimate $T_g$ was found on the return. The residual reaction heat was estimated from the nonreversible heat flow curve. The residual reaction heat was assumed to be due to the epoxy reaction. The conversion was calculated from the residual heat flow divided by the total heat of reaction. The heat of reaction was 502 J/g for DGEBA,[25,26] and that of PEG200DA was 532 J/g.[27]

### Rheology

The rheological properties of the rectangular specimens were determined in a TA Instruments AR2000

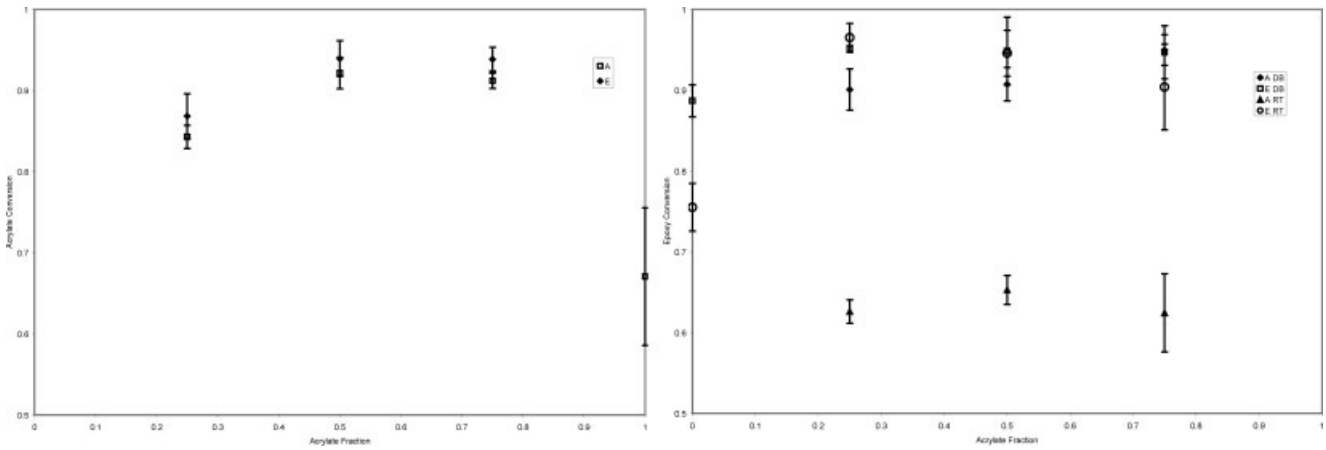


**Figure 2** (a) Acrylate conversion by FTIR as a function of the acrylate mass fraction and reaction sequence. (b) Epoxy conversion by FTIR as a function of the acrylate mass fraction, reaction sequence, and sample geometry. In this figure, A denotes acrylate-first samples, and E represents epoxy-first samples. DB (dogbone) and RT (rectangular) refer to sample geometry. The combination E DB denotes an epoxy-first dogbone sample for tensile testing.

rheometer. The temperature was reduced to −10°C and ramped to 200°C at 5°C/min. The strain was controlled at 0.02%, and the angular frequency was set at 6.284 rad/s during the test.

The rheology traces were processed with the Rheology Advantage Data Analysis program from TA Instruments. $G'$, the loss modulus ($G''$), and tan δ were measured. $T_g$ was estimated from the peak in the tan δ curve. $G'$ and tan δ at $T_g$ were recorded for further analysis.

### Mechanical properties

We determined the tensile properties of the dogbone specimens by testing in an Instron 4411 universal testing machine (Instron Corp., Norwood, MA) by clamping the sample with a jaw separation distance of 19.05 mm. A crosshead speed of 1.27 mm/min was used to pull the sample to failure.

Data collection and analysis and control of the testing machine was performed with the Instron Series IX Automated Materials Tester version 8.15.00 program by Instron Corp. This program calculated $E$, yield, and failure stress and strain for each trial.

Shore A hardness of the tensile samples was measured with a Pacific Instruments (Los Angles) model 306 hardness tester.

### Morphology

Digital photographs of the specimens were taken with a Nikon CoolPic 3100 camera. The rupture surfaces of the tensile samples were examined with an optical stereo microscope (Nikon SMZ 1500). A digital camera (Diagnostic Instruments, Inc., 11.2 Color Mosaic) was used to create image files for further analysis.

Samples for SEM were prepared by freezing in liquid nitrogen and then fracturing. The samples were mounted on a stub and sputter-coated with 200 Å of gold before imaging. A Jeol Limited scanning electron microscope model 840A (Tokyo) operated at 20 kV was used for imaging. A series of images were captured at magnifications from 500 to 15,000× with the IXRF systems (Houston, TX) integrated EDS system softwares.

## RESULTS

The use of ATR FTIR, pDSC, and mDSC allowed independent measurements of conversion, initial and final $T_g$ by composition, reaction sequence, and sample geometry. The methods of sample preparation were the same regardless of sample geometry, so it was anticipated that sample geometry would not affect the results. This was the case for all of the samples with the exception of the acrylate-first samples for rheometry, which resulted in lower epoxy conversions than expected.

The ATR FTIR data indicated that the acrylate conversion peaked at intermediate concentrations, as shown in Figure 2(a). In this and subsequent figures, the error bars represent a 95% confidence interval for the mean. When the acrylate was reacted first, the conversion was consistently slightly higher than when the epoxy was reacted first. The dilution of the acrylate extended the mobility, which allowed the reaction to go to a higher conversion. The decline in conversion at the lowest acrylate fraction represented a further shift, as time for diffusion and propagation approached the free-radical lifetime. In contrast, the conversion of the pure acrylate was limited by mobility as it crosslinked.

Similar to the acrylate conversion, there was slightly higher epoxy conversion at intermediate concentra-

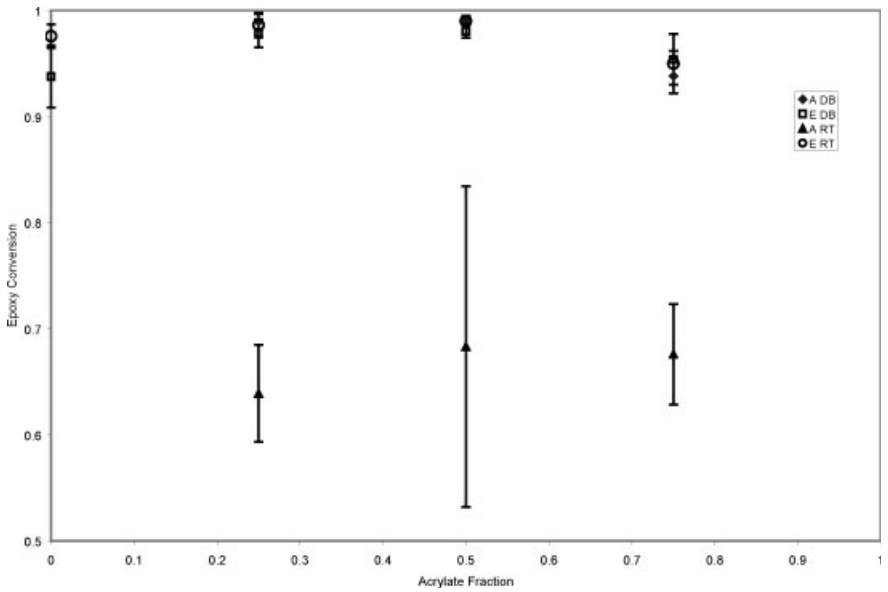


**Figure 3** Epoxy conversion from mDSC as a function of the acrylate fraction and reaction sequence. Similar to Figure 2, A denotes acrylate-first samples, and E represents epoxy-first samples. DB (dogbone) and RT (rectangular) refer to sample geometry. The combination E DB denotes an epoxy-first dogbone sample for tensile testing.

tions, with the exception of the acrylate-first rheometry samples [Fig. 2(b)]. In this and subsequent figures, the following nomenclature is used. The first letter denotes the reaction sequence with A for acrylate first and E for epoxy first. The following letters, if any, determine sample type with RT for rectangular samples for rheology testing and DB for dogbone samples for tensile testing. For example, the designation E DB denotes epoxy-first dogbone samples for tensile testing. The decline in conversion for the epoxy homopolymer was not as large as that of the acrylate homopolymer. The living nature of the propagating cation may have been the source of the extended polymerization of the epoxy. Like the acrylate, the epoxy also typically went to a higher conversion when an IPN was formed. This higher conversion of both components in the IPN was in contrast to previous studies.[10,11] However, these findings were consistent with our previous study, in which lower reaction rates and higher final conversions were observed during IPN formation with this model system.[28] The epoxy polymerization mechanism in this system was different than that in previous studies with epoxy amine and epoxy anhydride systems. The extent of the reaction in living cationic epoxy polymerizations could depend on the time after initiation, even after samples are cooled to room temperature. Propagation by an activated chain end requires the diffusion of monomer to the active end of the polymer chain.[25] Less molecular coordination is needed in these systems than in the addition reactions of epoxy amine and epoxy anhydride systems.

To check for residual acrylate reaction, the samples were evaluated by pDSC, and no appreciable reaction was observed on illumination at 30°C. This suggested complete acrylate conversion but could have also been due to sample vitrification, immeasurably slow polymerization rates, or consumption of the free-radical initiator.

Epoxy conversion from residual reaction heat estimated from nonreversible heat flow in the mDSC thermograph is shown in Figure 3 as a function of the acrylate mass fraction and reaction sequence. The trends correlated well with the epoxy conversion by FTIR [Fig. 2(b)], although small quantitative discrepancies were present. The observed discrepancy may have been partly due to the assumption that the residual heat represented the complete conversion of the epoxy monomer to polymer. In some cases, the DSC overestimated conversion when compared to the FTIR. This could have been due to vitrification reducing the residual reaction heat. Most of the overestimated conversions compared to FTIR were for the pure epoxy samples. The lower epoxy conversions occurred at various acrylate concentrations when the acrylate was reacted first. In these cases, the preformed acrylate network was either hindering the complete epoxy polymerization or segregating the epoxy into isolated domains so complete conversion could not be achieved.

In contrast to the correlation between epoxy conversion by FTIR and residual reaction enthalpy, the correlation of conversion from residual reaction enthalpy to acrylate conversion by FTIR was poor. As noted previously, the reaction heats for the monomers were very close to each other. If the residual reaction heat was due to acrylate polymerization, there should have been a correlation to the FTIR measured conversion.

With mDSC, an initial and final $T_g$ was determined from the reversible heat flow or heat capacity inflec-

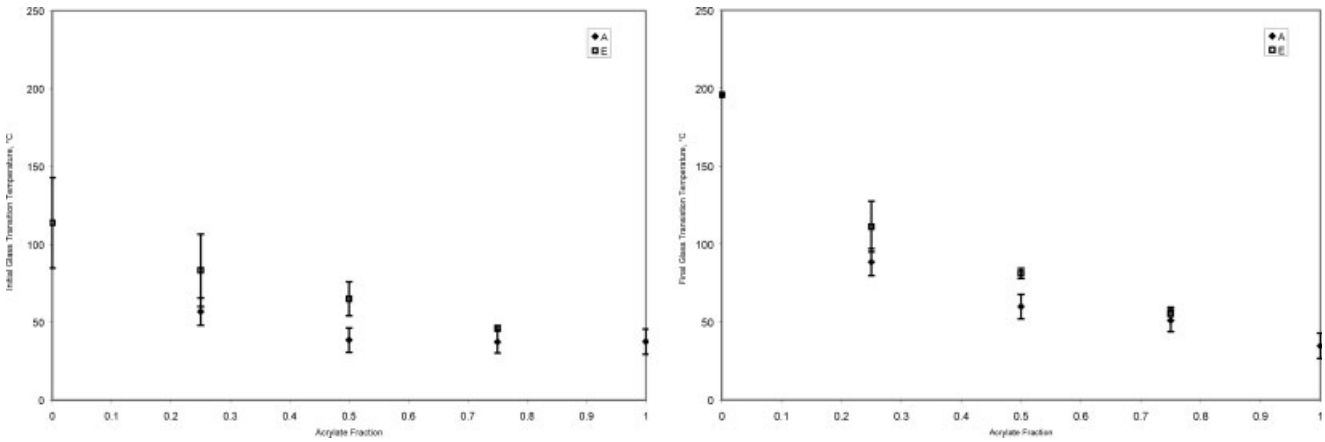


**Figure 4** (a) Initial and (b) final $T_g$ from mDSC as a function of the acrylate mass fraction and reaction sequence.

tion points. The epoxy polymerization was autocatalytic and thermosetting. mDSC had an advantage over conventional DSC in these cases as the reversible (phase transition) heat flows could be separated from the nonreversible (residual reaction) heat flows. Here, the initial $T_g$ was determined from an inflection in the reversible heat flow as the temperature was modulated and ramped to the final test temperature (300°C). The final $T_g$ was estimated from an inflection in the reversible heat flow during the cool down ramp and modulation. This final $T_g$ should have been representative of the ultimate $T_g$, as the high temperature would have allowed the complete reaction. Initial $T_g$ increased with epoxy concentration, as shown in Figure 4(a). The initial $T_g$ was higher when the epoxy was reacted first. The final $T_g$ also increased sharply with epoxy content, as shown in Figure 4(b). The epoxy-first samples had higher final $T_g$'s. The lower $T_g$'s for the acrylate-first polymerizations were indicative of incomplete polymerization of the epoxy. This may have been due to vitrification or isolation of the epoxy in domains so that complete conversion was not possible.

Initial and final $T_g$ values were compared to conversion determined by FTIR. With the exception of the pure epoxy samples, the initial $T_g$ increased with epoxy conversion. Initial $T_g$ was a stronger function of acrylate mass fraction than acrylate conversion. The relationship of final $T_g$ to conversion was less clear. The final $T_g$ appeared to be a stronger function of composition than conversion. This was to be expected, as the measured final $T_g$ was after the additional conversion had occurred. Regression analysis confirmed these observations.

## Rheology

The tan δ at peak value was higher when the acrylate was reacted first, as shown in Figure 5. The peak was

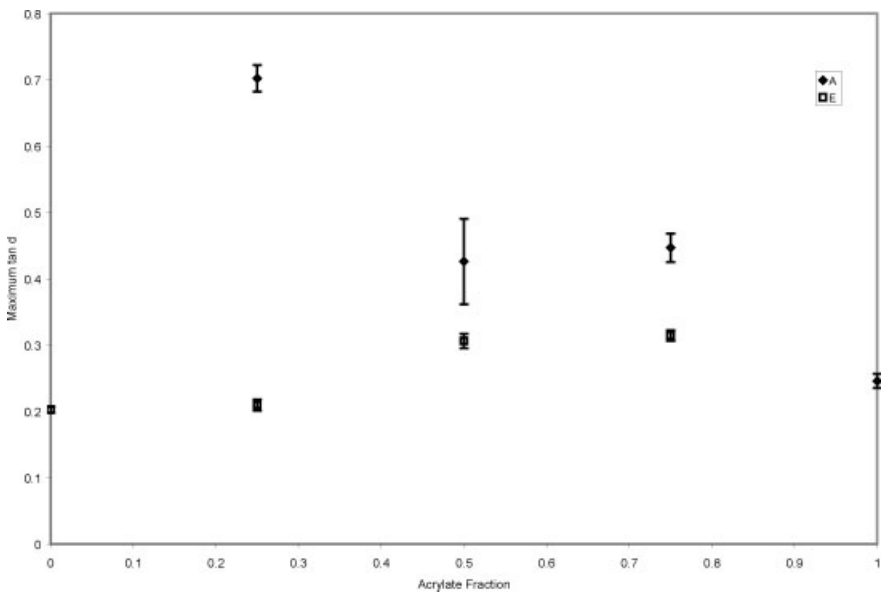


**Figure 5** Tan δ at peak as a function of the composition and reaction sequence.

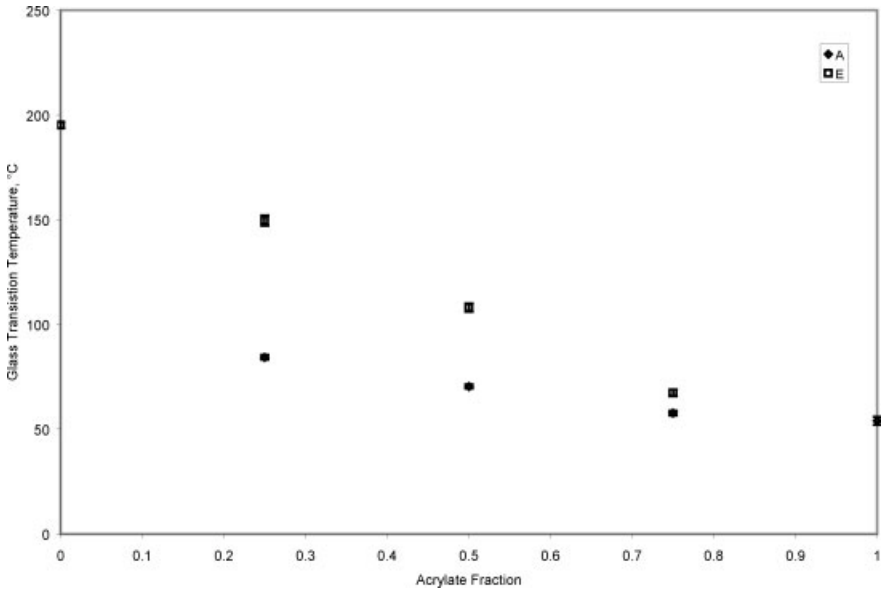


**Figure 6** $T_g$ determined by rheometry as a function of the acrylate mass fraction and reaction sequence.

also higher at intermediate compositions between the homopolymers. Maximum damping occurred with the 0.25 acrylate fraction sample when the acrylate was reacted first. This was in contrast to the epoxy-first sample of the same composition, which showed nearly the same damping as the epoxy homopolymer and indicated little synergy due to the inclusion of the acrylate.

$G'$ at the tan δ peak was insensitive to the reaction sequence and composition and was uniform at about 40 MPa except for the pure epoxy samples (data not shown). Acrylate-modified systems had lower moduli at the tan δ peak than the epoxy homopolymer. This corresponded to a more rubbery system, which was in qualitative agreement with the $T_g$ estimates.

The peak in the tan δ curve from rheology measurements was also used to estimate $T_g$ (Fig. 6). Similar to the mDSC estimates, $T_g$ for epoxy-first samples was much higher than that of the acrylate-first samples. This provided further evidence of differences in the microstructure of the IPNs due to the reaction sequence.

Initial and final $T_g$'s from mDSC were compared to the $T_g$ estimated from rheometry. The $T_g$ from rheometry was much closer to the final $T_g$ from mDSC. In both of these cases, the epoxy reaction continued as

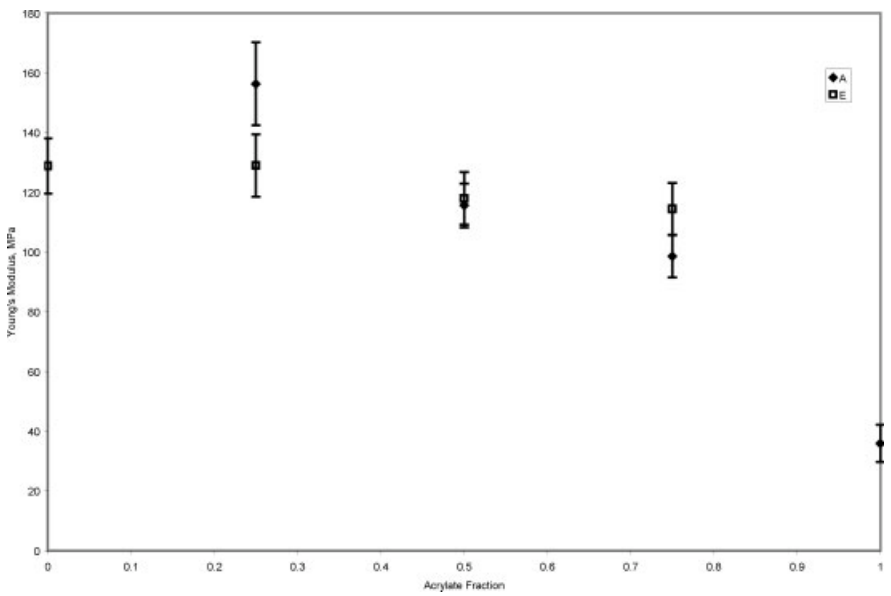


**Figure 7** Composition and reaction sequence effects on $E$.

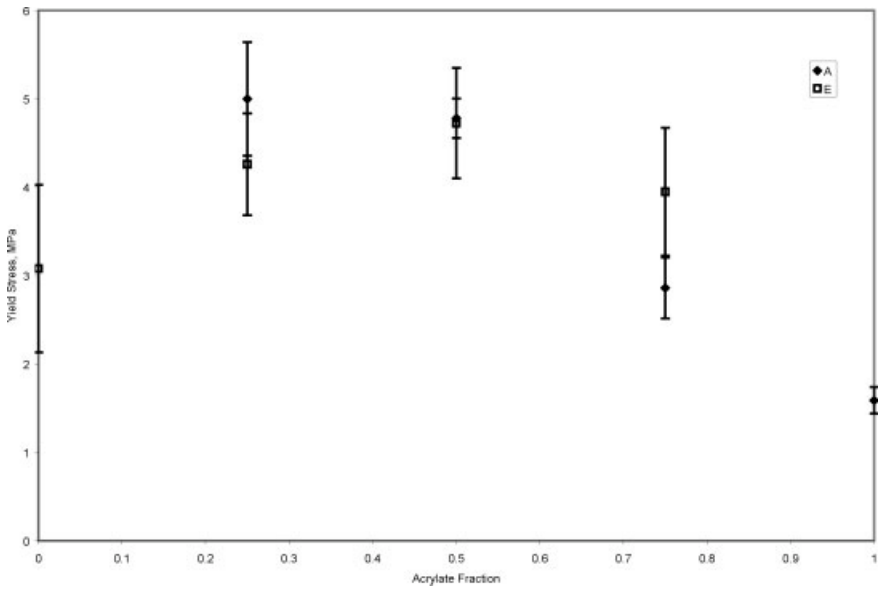


**Figure 8** Acrylate mass fraction and reaction sequence effects on yield stress.

the temperature was ramped. The $T_g$ estimates from rheometry were more consistent compared to mDSC estimates and were generally higher.

### Mechanical properties

From the tensile test, $E$ was calculated, as shown in Figure 7. The results indicate that the addition of epoxy strengthened the material. The modulus quickly increased to a limiting value (i.e., that of pure epoxy) with the slight addition of epoxy. The modulus was relatively independent of the reaction sequence. Up to 0.25 acrylate fraction, the acrylate-first samples had a slightly lower $E$ than the epoxy-first samples. The acrylate-first samples at 0.25 acrylate fraction were also the most opaque samples (as observed by digital photography) and had the highest tan δ peak value.

The yield stress showed a maximum with IPN formation at intermediate concentrations, as depicted in Figure 8. The peak position was weakly dependent on the reaction sequence. The addition of the acrylate toughened the epoxy. The peak in the yield stress occurred at 0.25 acrylate fraction when the acrylate was reacted first. This was the maximum toughness of the network.

There was no clear relationship between the yield stress and initial $T_g$. The yield stress increased with final $T_g$ to the peak yield stress and then declined as

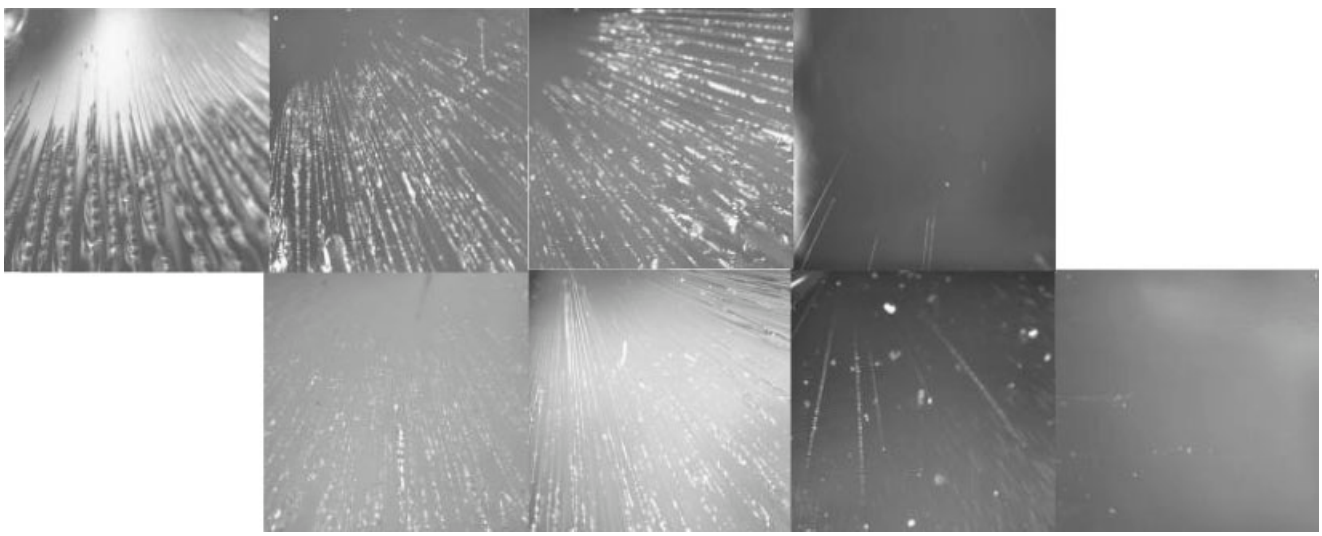

**Figure 9** Rupture surfaces of the tensile samples at 8.4×. The top row shows the epoxy-first samples; from left to right, the acrylate mass fractions are 0, 0.25, 0.50, and 0.75. The bottom row shows the acrylate-first samples from 0.25 to 1.0 acrylate fraction. The actual image size was approximately 2.5 × 2.5 mm.

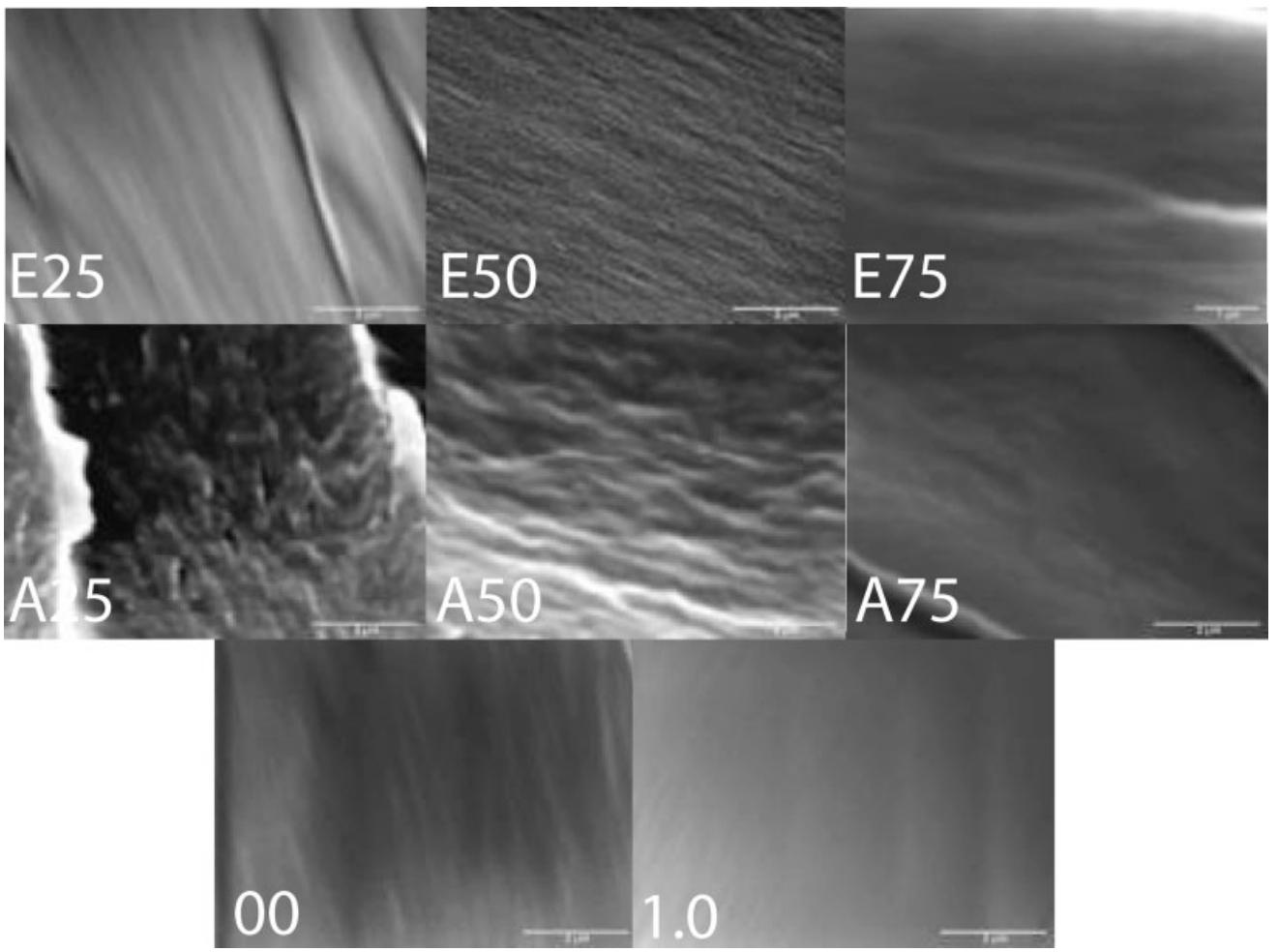


**Figure 10** SEM images of IPNs and homopolymer samples by composition and reaction sequence. The reaction sequence is denoted by the first letter, with E for epoxy first and A for acrylate first. The numbers refer to the acrylate percentage, with the exception that 1.0 is 100% acrylate.

the final $T_g$ reached that of the epoxy homopolymer. This may have been due to the dependence of yield stress and final $T_g$ on composition and reaction sequence.

The yield strain increased monotonically with acrylate concentration when the epoxy was reacted first (data not shown). The increase was not as linear for the acrylate-first samples, with a deviation at 0.75 acrylate fraction. The epoxy homopolymer had the lowest strain at yield.

The surface hardness of the material decreased monotonically with acrylate fraction (data not shown). The reaction sequence did not have a significant effect on the hardness. Because hardness is a surface property, it may not affect the bulk material properties. The hardness increased with initial $T_g$ and approached a limiting value.

### Morphology

Microscopic evaluation of the rupture surface of the tensile samples revealed increasingly brittle material as the samples progressed from pure acrylate to pure epoxy, as shown in Figure 9. Brittleness was indicated by the density of the crack lines on the rupture surface. The brittleness of the samples also depended on the reaction sequence, with acrylate-first samples being less brittle. This was consistent with the lower $E$ and yield stress reported earlier.

The SEM images exhibited increasing coarsening with acrylate-first samples up to 0.25 acrylate fraction, as shown in Figure 10. No apparent microstructure was visible for the epoxy-first samples or the homopolymers. The initial and final $T_g$ from mDSC supported a different microstructure for the acrylate-first samples when compared to the epoxy-first samples.

## DISCUSSION

Polymer material properties are often modeled as functions of conversion or $T_g$. The presence of more than one $T_g$ is often used as evidence of multiple phases.[4] Comparisons were made between the differ-

ent conversion estimates and between the initial and final $T_g$ and material properties. The conversion estimated by residual reaction heat from mDSC correlated well with the epoxy conversion estimated by ATR FTIR but did not correlate with the acrylate conversion by ATR FTIR. The initial $T_g$ correlated to the epoxy conversion, but neither $T_g$ correlated to acrylate conversion. The $T_g$ estimated from rheometry correlated well with the final $T_g$ by mDSC and somewhat weakly to the initial $T_g$. In all cases, only one $T_g$ was evident by rheometry. There appeared to be a relationship between $E$, yield stress, and hardness with the initial and final $T_g$'s. These apparent relationships may have been due to the dependence of $T_g$ on the acrylate fraction. The lack of clear correlations between these variables could have also been due to the lack of spread in the data. During these experiments, the samples were reacted under conditions to achieve full conversion. Therefore, there was limited spread in the conversions and the subsequent sample $T_g$'s.

The effects of two variables, acrylate fraction and reaction sequence, on the conversion, $T_g$, rheological properties, and mechanical properties were systematically explored. The responses can be separated into those that were only dependent on composition and those that were dependent on both variables. A number of responses were dependent only on composition. The conversions of acrylate and epoxy, whether measured by ATR FTIR or DSC, showed maxima at intermediate compositions when IPNs were formed. This was attributed to the dilution effect, which allowed continued mobility of reacting species. This was the case, even though the reaction mechanisms were different. At high conversions, both polymerizations became dependent on the diffusion of the monomer to the active chain ends. $E$ and $G''$ displayed limiting-value behavior at intermediate compositions. $E$ quickly approached that of the epoxy homopolymer. This was in contrast to the approximately linear composition dependent modulus[9,12] and tensile strength[12] reported in other works or a modulus that remained close to the rubber phase for compositions up to 40% rubber content.[14] In this study, the presence of an epoxy network, regardless of how complete or uniform, immediately increased $E$. In contrast, $G'$ at the tan δ peak remained close to that of the acrylate polymer and was lower than that of the epoxy polymer. The acrylate network dominated $G'$. The acrylate network absorbed energy and dissipated it as heat, thus limiting the energy storage capacity. Hardness and yield strain changed monotonically in opposite directions with composition. Hardness increased with epoxy concentration, whereas the yield strain increased with acrylate fraction, which suggested that the acrylate network elongated to relieve the stress.

Responses that changed with both reaction sequence and composition were $T_g$, tan δ peak, yield stress, and morphology. $T_g$ increased linearly with acrylate fraction. There was a large difference in $T_g$ by reaction sequence. The largest difference, 75°C, was at 0.25 acrylate fraction. This large $T_g$ separation was consistent with the largest degree of phase separation as evidenced by coarsening in SEM micrographs and the opacity of acrylate first samples at low acrylate mass fraction. The acrylate network disrupted the formation of a uniformly continuous epoxy network. The acrylate-first samples also deviated from a simple linear mixing rule. This suggested the formation of a different phase or at least a change in the composition of the continuous phase. The tan δ at peak was a complex function of composition and reaction sequence. The tan δ at peak was larger for IPNs than the homopolymers because the synergy from IPN formation aided in damping. In addition to the peaks being higher, the peaks were broader, which indicated energy absorption over a wider temperature range. In a similar system, poly(ethylene glycol) diacrylate (PEGDA) with DGEBA and diamine, the epoxy copolymer had the largest tan δ peak. All of the samples had one tan δ peak, yet the scanning electron micrographs indicated phase separation at acrylate fractions greater than 50%.[8] Dean et al.[29] reported one or two $T_g$'s depending on the reaction sequence for IPNs; however, their work also indicated incomplete conversion of both components. The yield stress peaked with IPN formation due to the maximum entanglement of networks and higher conversions and was weakly dependent on the reaction sequence. Higher conversions resulted in a higher network crosslink density. In the IPNs, the acrylate network toughened the epoxy, increasing the yield strength. The maximum yield stress and tan δ peak were consistent with the electron microscopy studies for the acrylate-first samples at 0.25 acrylate fraction. However, the epoxy-first IPNs also showed improved properties relative to the homopolymers and were not largely different from the acrylate-first samples in most cases. This suggested that the morphology played a key role in the final properties. However, IPN formation, with or without evident morphology, was also important to the final properties.

This systematic study of IPN formation at different compositions and processing conditions yielded new details and some unanticipated results on the role of these variables on structure and physical properties. In this model system, the reaction rates were rapid enough to prevent significant phase separation, as evidenced by minimal morphology development, yet significant changes in material properties resulted from changes in processing. The material property response for this model system was often in disagreement to previously reported responses based on simple mixing-rule-type models. For example, the behavior for $E$ in this system followed an upper bound pattern in contrast to the lower bound patterns previously reported in the literature. These findings highlight the need for consistent and repeatable processing conditions for the achieve-

ment of reliable material properties. This sensitivity to processing can also be exploited to tailor material properties for specific applications, whereas presenting an additional challenge for material design as an additional dimension, which is not frequently considered, is added to the design space.

We demonstrated that the preferential formation of one polymer network before the other in this IPN system dictated the material properties and was just as important as the composition. Common mixing rules used to predict material properties did not account for differences in processing conditions impacting material properties. Furthermore, the proper mixing rule to use was not known *a priori* and changed depending on properties. A good fit to a mixing model is often used as evidence for phase composition and morphology.[30] These findings highlight the need for a comprehensive investigation of these systems so that a framework for material property prediction can be developed for these complex materials.

## CONCLUSIONS

Acrylate/epoxy IPN samples were formed over a range of compositions and with different reaction sequences. The conversion, physical properties, and morphology of these samples were investigated with a variety of techniques. The relationships between the morphology and material properties of acrylate/epoxy IPNs at different compositions and reaction sequences were complex and nonlinear. Large differences in material properties were observed due to changes in processing conditions with concurrently minimal morphology development. The makes the *a priori* prediction of phase morphology and physical properties of IPNs very difficult. New modeling approaches that account for these complexities are necessary to understand IPN structure–property–processing relationships.

## References


1. Sperling, L. H. In Multicomponent Polymer Materials; Paul, D. R.; Sperling, L. H., Eds.; American Chemical Society: Philadelphia, 1984; p 21.
2. Utracki, L. A. In Interpenetrating Polymer Networks; Klempner, D.; Sperling, L. H.; Utracki, L. A., Eds.; American Chemical Society: New York, 1994; p 77.
3. Suthar, B.; Xiao, H. X.; Klempner, D.; Frisch, K. C. Polym Adv Technol 1996, 7, 221.
4. Yang, J.; Winnik, M. A.; Ylitalo, D.; Devoe, R. J. Macromolecules 1996, 29, 7047.
5. Laskar, J.; Vidal, F.; Fichet, O.; Gauthier, C.; Teyssie, D. Polymer 2004, 45, 5047.
6. Król, P.; Wojturska, J.; Statyukha, G. A.; Skladannyy, D. M. J Appl Polym Sci 2005, 97, 1855.
7. Lin, M.-S.; Jenc, K.-T.; Huanc, K.-Y.; Shih, Y.-F. J Polym Sci Part A: Polym Chem 1993, 31, 3317.
8. Lin, M.-S.; Jeng, K.-T. J Polym Sci Part A: Polym Chem 1992, 30, 1941.
9. Lin, M.-S.; Lee, S.-T. Polymer 1997, 38, 53.
10. Lin, M.-S.; Lee, S.-T. Polymer 1995, 36, 4567.
11. Dean, K.; Cook, W. D. Macromolecules 2002, 35, 7942.
12. Tan, S.-S.; Zhang, D.-H. Acta Polymer 1996, 47, 219.
13. Karger-Kocsis, J.; Gryshchuk, O.; Jost, N. J Appl Polym Sci 2003, 88, 2124.
14. Das, B.; Chakrabarty, D.; Hajra, A. K.; Sinha, S. J Appl Polym Sci 1994, 53, 1491.
15. Karger-Kocsis, J.; Gryshchuk, O.; Schmitt, S. J Mater Sci 2003, 38, 413.
16. Boey, F. Y. C.; Chia, N. K.; Rath, S. K.; Abadie, M. J. M. J Appl Polym Sci 2001, 82, 3099.
17. Gryshchuk, O.; Karger-Kocsis, J. J Polym Sci Part A: Polym Chem 2004, 42, 5471.
18. Rogovina, L. Z.; Dembo, A. T.; Sharma, P. R. S.; Frisch, H. L.; Schulz, M. Polymer 2000, 41, 2893.
19. Nakanish, H.; Satoh, M.; Norisuye, T.; Tran-Cong-Miyata, Q. Macromolecules 2004, 37, 8495.
20. Alcântara, R. M.; Pires, A. T. N.; Barros, G. G. D.; Belfiore, L. A. J Appl Polym Sci 2003, 89, 1858.
21. Jansen, B. J. P.; Ragosta, S.; Meijer, H. E. H.; Lemstra, P. J. Macromolecules 1999, 32, 6290.
22. Jeong, Y. G.; Hashida, T.; Hsu, S. L.; Paul, C. W. Macromolecules 2005, 38, 2889.
23. ASTM D 5279-01; American Society for Testing and Materials: West Conshohocken, PA, 2001; p 1.
24. Standard Test Method for Plastics: Dynamic Mechanical Properties: In Torsion, D 5279-01, American Society for Testing and Materials, West Conshohocken, PA, 2001.
25. Standard Test Method for Tensile Properties of Plastics, D 638-03, American Society for Testing and Materials, West Conshohocken, PA, 2004.
26. Crivello, J. V.; Kong, S. Macromolecules 2000, 33, 833.
27. Pappas, S. P. In Topics in Applied Chemistry; Pappas, S. P., Ed.; Plenum: New York, 1992; p 1.
28. Nowers, J. R.; Narasimhan, B. Polymer 2006, 47, 1008.
29. Dean, K.; Cook, W. D.; Rey, L.; Galy, J.; Sautereau, H. Macromolecules 2001, 34, 6623.
30. Mathew, A. P.; Packirisamy, S.; Thomas, S. J Appl Polym Sci 2000, 78, 2327.